ISBN: 978-3-95450-223-3 ISSN: 2673-7000 doi:10.18429/JACoW-NAPAC2019-MOPLM21

CIRCUIT MODEL ANALYSIS FOR HIGH CHARGE IN THE APS PARTICLE ACCUMULATOR RING*

K.C. Harkay†, J.R. Calvey, J.C. Dooling, L. Emery, R.R. Lindberg, K.P. Wootton, C. Yao
Argonne National Laboratory, Lemont, IL 60439, USA

Abstract

The Advanced Photon Source (APS) particle accumulator ring (PAR) was designed to accumulate linac pulses into a single bunch with a fundamental rf system, and longitudinally compress the beam with a harmonic rf system prior to injection into the booster. For APS Upgrade, the injectors will need to supply full-current bunch replacement with high single-bunch charge for swap-out in the new storage ring. Significant bunch lengthening, energy spread, and synchrotron sidebands are observed in PAR at high charge. Lower-charge dynamics are dominated by potential well distortion, while higher-charge dynamics appear to be dominated by microwave instability. Before a numerical impedance model was available, a simple circuit model was developed by fitting the measured bunch distributions to the Haissinski equation. Energy scaling was then used to predict the beam energy sufficient to raise the instability threshold to 18-20 nC. With the beam in a linear or nearly linear regime, higher harmonic radio frequency (rf) gap voltage can be used to reduce the bunch length at high charge and better match the booster acceptance.

INTRODUCTION

The APS Upgrade (APS-U) currently under production is based on reverse-bend multibend achromat optics [1,2]. One of the consequences of the 1-2 orders of magnitude reduction in the horizontal emittance is a much-reduced transverse acceptance, which will require on-axis injection. The most straightforward on-axis injection scheme is swap-out, where the injectors produce enough single-bunch charge to perform complete bunch replacement. This presents a challenge for the injector [3].

The plan is to meet the APS-U injection requirements through upgrades of the injector complex, while keeping the basic structure. The linac provides 1-nC pulses at a 30-Hz rate. Up to 20 pulses are accumulated and damped in the particle accumulator ring (PAR) [4] at the fundamental rf frequency of 9.776 MHz. In the final 230 ms of the 1-s cycle, the single bunch is captured in a 12$^{\text{th}}$ harmonic rf bucket and the bunch length is further compressed. The bunch is injected into the booster where it is ramped to full energy and extracted into a transport line that was redesigned for matching into the MBA storage ring (SR) [5].

The PAR was designed for a maximum charge of 6 nC, and needs to provide up to 20 nC in a single bunch for APS-U. Lower-charge dynamics are dominated by potential-well distortion (PWD), while higher-charge dynamics are dominated by microwave instability. Significant bunch lengthening and synchrotron sidebands are observed at high charge. PAR bunch lengths above ~650 ps rms result in unacceptably low injection efficiency into the booster (high beam loading is also a concern in booster [3,6]). Figure 1 shows various measurements in PAR of charge accumulation and charge-dependent bunch distributions [7], bunch length, and longitudinal bunch spectra at high charge after compression (~900 ms in cycle). Spectra at 375, 425, and 450 MeV indicate a more stable beam at higher energy. An impedance model based on numerical computation was recently completed [8], and will be used to simulate the instability. In the meantime, a simple circuit model was used to predict the beam energy needed to raise the instability threshold such that the bunch length can be compressed to ~650 ps at 20 nC full charge.

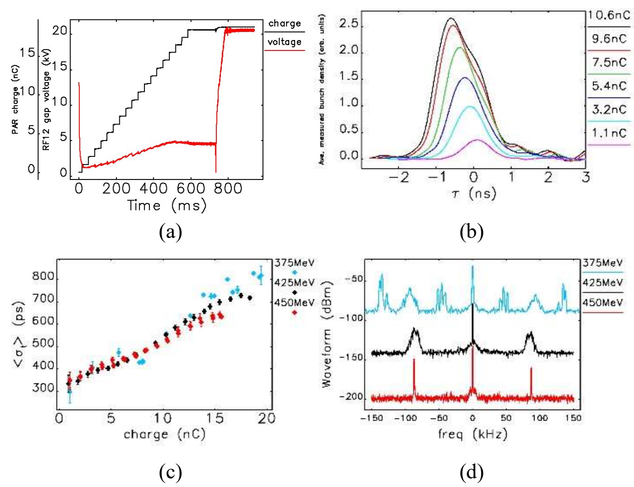

Figure 1: PAR measurements: (a) charge and harmonic rf waveform over cycle, (b) bunch distributions, (c) rms bunch length, and (d) synchrotron tune spectra for 16nC.

CIRCUIT MODEL ANALYSIS

Assuming that the low-charge dynamics is predominantly in the PWD regime, equilibrium bunch density distributions were computed using the Haissinski equation [9] in a dual rf system and a circuit model for the impedance. The code uses expressions in Bane *et al* [10,11]. The code was generalized to model both a main and higher-harmonic rf potential; the harmonic can be phased for either bunch shortening, as in PAR, or for bunch lengthening.

Fit results using bunch duration monitor (BDM) [7] measurements at 425 MeV are shown in Fig. 2. The initial analysis assumed no energy spread growth in a pure PWD regime. Circuit model reactance Z/n = 25 Ω and resistance R = 1300 Ω gave the best fit for both the bunch length and bunch shape “leaning” towards the head of the bunch (to-

* Work supported by U. S. Department of Energy, Office of Science, under Contract No. DE-AC02-06CH11357.
† harkay@anl.gov.

ISBN: 978-3-95450-223-3 ISSN: 2673-7000 doi:10.18429/JACoW-NAPAC2019-MOPLM21

wards the left in the plots). Given the non-Gausssian distortion of the bunch at higher charge, the full width half max (FWHM) is the more relevant parameter to fit.

The bunch lengthening slope changes (increases) above a threshold charge of ~10 nC (Fig. 3). The FWHM bunch length was divided by 2.35 to approximate the rms value. Since only constant natural energy spread was included in the analysis, the Haissinski distributions are only valid in the PWD regime; a slope change would suggest the onset of a microwave instability. The synchrotron spectra show the expected detuning at lower charge, shown in Fig. 4. However, a sudden jump is observed at a threshold bunch charge that is energy dependent. The threshold is ~10 nC (~7 nC) for 425 (375) MeV, which matches the charge at which the bunch lengthening slope changes in Fig. 3 (1c).

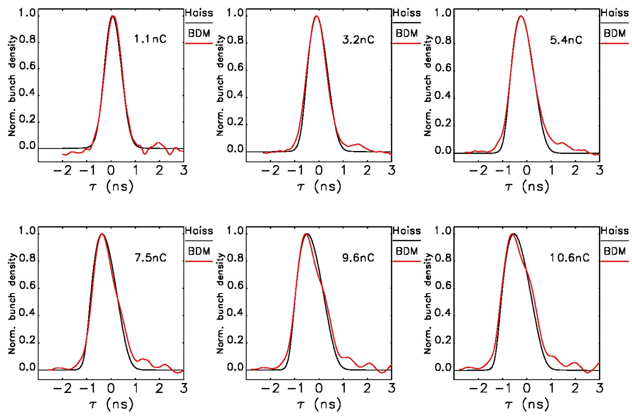

Figure 2: Haissinski fits to measured beam distributions.

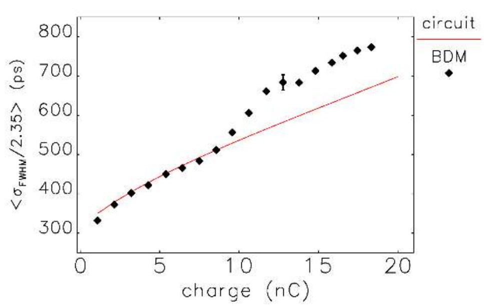

Figure 3: Bunch length comparisons of measurements and circuit model for 425 MeV, using natural energy spread.

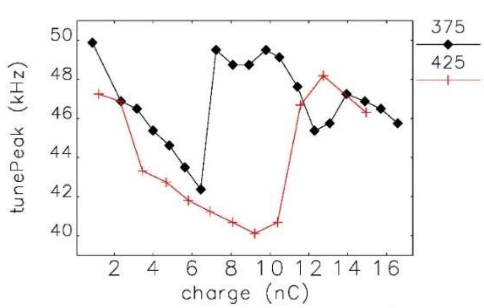

Figure 4: Measured synchrotron tune peak frequency vs. charge at two beam energies.

Test of Linear Regime

The PWD regime should exhibit bunch length dependence on harmonic rf voltage. This was tested in PAR over a range, from the nominal value of 20 kV to the maximum value of 24 kV, limited by the rf amplifier. Over this limited range, the measured variation of the bunch length is consistent with predictions of the circuit model at low charge, shown in Fig. 5. The bunch length shows rf voltage dependence even somewhat beyond the 10-nC threshold, even though it deviates from the circuit model.

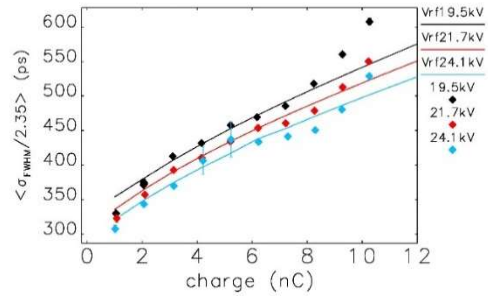

Figure 5: Variation of bunch length with harmonic rf voltage after compression; comparison of circuit model (lines) with measurements (symbols).

Energy Scaling

Higher beam energy, E, helps in two ways: the natural (zero-current) relative energy spread, δ_E, increases with energy, which increases Landau damping, and the instability growth rates scale with E^{-1}. In general, we can assume that the instability threshold charge scales like [12]

$$Q_{th} \propto E\delta_E^2\sigma_{t,th}$$

where Q_{th} is bunch charge and $\sigma_{t,th}$ is the bunch length at the threshold. Table 1 shows PAR parameters used for the scaling. The radiation damping time, τ_E, is shown for reference. The measured charge and bunch length thresholds for 375 MeV and 425 MeV are consistent with the theoretical scaling. The Q_{th} values for 450, 475, and 500 MeV were computed using the scaling rule (shown in **bold**), assuming the 650-ps bunch length goal. This suggests that at 500 MeV, the threshold charge is 20-22 nC, and at 475MeV, the threshold charge is 18-20 nC.

Table 1: PAR Parameters for Energy Scaling

Energy (MeV)	δ_E ($\times10^{-4}$)	τ_E (ms)	Q_{th} (nC)	$\sigma_{t,th}$ (ps)
375	3.42	25.8	6-7	450
425	3.88	17.8	10-11	550
450	4.10	14.9	**15-17**	**650**
475	4.33	12.7	**18-20**	**650**
500	4.56	10.9	**20-22**	**650**

Under the assumption that the energy scaling is valid, and that the bunch lengthening below threshold can be estimated using the circuit model, we can estimate the bunch length for higher gap voltage. The results are shown in Fig. 6. Calculations for 500 MeV suggest that 30 kV gives ~600 ps rms bunch length at 20 nC, which provides some margin. The present linac can deliver 450 MeV, and there are plans for upgrading the energy to at least 500 MeV. The

North American Particle Acc. Conf. NAPAC2019, Lansing, MI, USA JACoW Publishing
ISBN: 978-3-95450-223-3 ISSN: 2673-7000 doi:10.18429/JACoW-NAPAC2019-MOPLM21

PAR harmonic rf amplifier is also being upgraded to provide 30 kV.

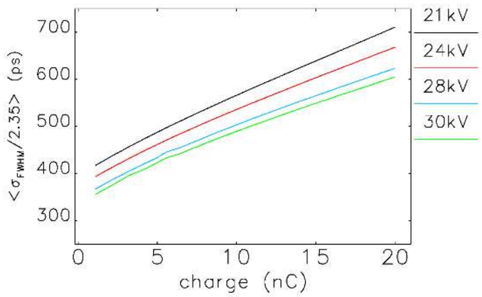

Figure 6: Bunch lengthening predictions for 500 MeV with higher harmonic gap voltage, using the circuit model.

Analysis Including Energy Spread

Recent diagnostics upgrades to two synchrotron light ports, one at low and one at high dispersion, allow determination of the energy spread and emittance from the measured horizontal beam sizes. It turns out that the longitudinal dynamics even at low charge are not strictly linear because the energy spread starts to grow at low charge; see Fig. 7. Furthermore, unlike a classical microwave instability, the energy spread does not increase monotonically with charge. Similar observations are reported at NSLS-II [13].

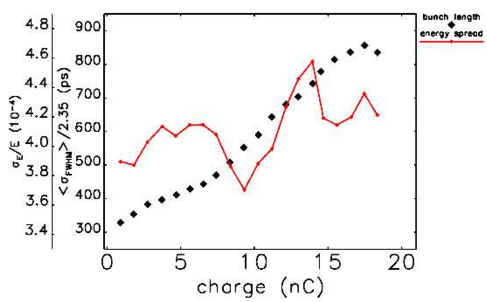

Figure 7: Bunch length and energy spread measured at the same time, 425 MeV.

The circuit model analysis was repeated to include the measured energy spread to compute the equilibrium distributions. For the first circuit model, only the low-charge distributions were fit. In the second model, an attempt was made to fit up to high charge. The results are shown in Fig. 8. The low charge data fit better with Z/n = 20 Ω and R = 800 Ω. The best fit to the full charge range gives Z/n = 15 Ω and R = 2300 Ω, but the deviations are large and the bunch shapes are not well matched (not shown).

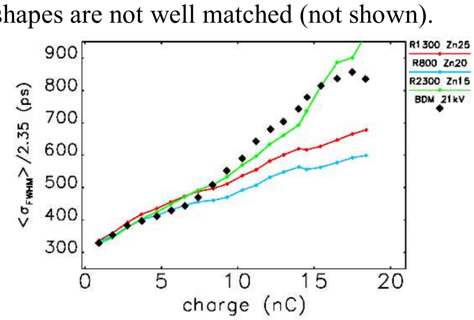

Figure 8: Bunch length comparisons of measured BDM data and circuit models for 425 MeV, using measured energy spread.

LIMITATIONS OF CIRCUIT MODEL

The circuit model cannot predict the microwave instability threshold with higher energy and a shorter bunch (with higher harmonic rf voltage). It also cannot be used directly to simulate the beam. One would need to define a cutoff frequency, whose choice is somewhat arbitrary. It is possible, however, to compare the circuit model results with the loss factor and the numerical PAR impedance (from [8]).

The loss factor was measured using two techniques. First, the beam phase shift as a function of charge was measured using rf diagnostics. A streak camera was also used to measure the change in the arrival time of the bunch vs charge. Both techniques gave a loss factor of about 170 V/nC for a 1-ns bunch. Assuming a constant real impedance, this gives an R of about 600 Ohm. This is comparable to the low-charge circuit model fit in Fig. 8.

To qualitatively compare the circuit model with the impedance [8], we compute a running average of the real part, and a running slope fit of the imaginary part divided by n (where n = f / 9.776MHz), shown in Fig. 9. The impedance exhibits sharp resonances around 800 MHz and 1600 MHz; this explains why the curves are not smooth. The low-charge circuit model is the same order of magnitude as the lowest-frequency average R (800 Ω vs. 950 Ω) and Z/n slope fit (20 Ω vs. 9 Ω); this is below the first resonance.

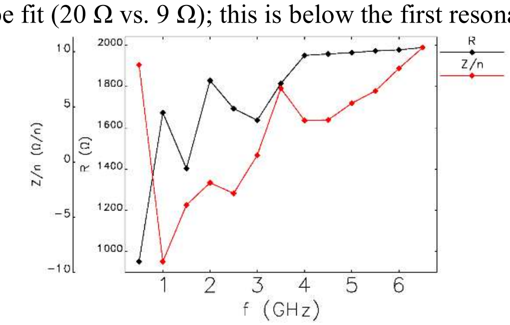

Figure 9: Running average of the real part, and running slope of the imaginary part divided by n, of the PAR numerical impedance in [8]. Frequency steps are 500 MHz.

CONCLUSION

Using a circuit model, higher beam energy and higher harmonic rf voltage are predicted to enable capture of a 20-nC bunch from PAR into the booster. The circuit model is roughly consistent with the recently completed numerical impedance model. Simulations using the impedance model are planned. The predictions will be compared with measurements made after upgrades to higher linac energy and a new harmonic rf amplifier.

ACKNOWLEDGEMENTS

The authors thank T. Berenc, U. Wienands, and the APS-U Injector and APS Operations teams for making these studies possible.

REFERENCES

[1] "Advanced Photon Source Upgrade Project Preliminary Design Report," Argonne, Lemont, IL, USA, 2017. doi:10.2172/1423830

ISBN: 978-3-95450-223-3 ISSN: 2673-7000 doi:10.18429/JACoW-NAPAC2019-MOPLM21

[2] M. Borland, T. G. Berenc, R. R. Lindberg, V. Sajaev, and Y. P. Sun, "Lower Emittance Lattice for the Advanced Photon Source Upgrade Using Reverse Bending Magnets", in *Proc. NAPAC'16*, Chicago, IL, USA, Oct. 2016, pp. 877-880. doi:10.18429/JACoW-NAPAC2016-WEPOB01

[3] K. C. Harkay *et al.*, "High-Charge Injector for on-Axis Injection Into A High-Performance Storage Ring Light Source", in *Proc. IPAC'19*, Melbourne, Australia, May 2019, pp. 3423-3426. doi:10.18429/JACoW-IPAC2019-THYYPLM3

[4] M. Borland, "Commissioning of the Argonne Positron Accumulator Ring", in *Proc. PAC'95*, Dallas, TX, USA, May 1995, paper FAR11, p. 287.

[5] A. Xiao and M. Borland, "Transport Line Design and Injection Configuration Optimization for the Advanced Photon Source Upgrade", in *Proc. IPAC'18*, Vancouver, Canada, Apr.-May 2018, pp. 1287-1289. doi:10.18429/JACoW-IPAC2018-TUPMF017

[6] J. R. Calvey, M. Borland, K. C. Harkay, R. R. Lindberg, and C. Yao, "Simulations of Booster Injection Efficiency for the APS-Upgrade", in *Proc. NAPAC'16*, Chicago, IL, USA, Oct. 2016, pp. 647-650. doi:10.18429/JACoW-NAPAC2016-WEA1CO03

[7] J. C. Dooling, J. R. Calvey, K. C. Harkay, B. X. Yang, and C. Yao, "Fast Photodetector Bunch Duration Monitor for the Advanced Photon Source Particle Accumulator Ring", in *Proc. IPAC'18*, Vancouver, Canada, Apr.-May 2018, pp. 1819-1822. doi:10.18429/JACoW-IPAC2018-WEPAF006

[8] C.-Y. Yao *et al.*, "Longitudinal Impedance Modeling of APS Particle Accumulator Ring with CST," presented at *NAPAC'19*, Lansing, MI, USA, Sep. 2019, paper MOPLM17.

[9] J. Haissinski, "Exact longitudinal Equilibrium Distribution of Stored Electrons in the Presence of Self-Fields," *Il Nuovo Cimento*, vol. 18, 1973, p. 72.

[10] K. L. F. Bane and R. D. Ruth, "Bunch Lengthening Calculations for the SLC Damping Rings", in *Proc. PAC'89*, Chicago, IL, USA, Mar. 1989, pp. 789-792.

[11] K. L. F. Bane, "Bunch Lengthening in the SLC Damping Rings," SLAC, Menlo Park, CA, USA, Report SLAC-PUB-5177, Feb. 1990.

[12] D. Boussard, "Observation of microwave longitudinal instabilities in the CPS," CERN, Geneva, Switzerland, Report LABII/RF/Int.75-2, 1975.

[13] A. Blednykh *et al.*, "New Aspects of Longitudinal Instabilities in Electron Storage Rings," *Scientific Reports,* vol. 8, 2018, p. 11918. doi: 10.1038/s41598-018-30306-y